



This is a repository copy of *Equivalent circuit parameter extraction of low-capacitance high-damping PTs*.

White Rose Research Online URL for this paper:
<https://eprints.whiterose.ac.uk/156350/>

Version: Accepted Version

Article:

Forrester, J., Li, L., Davidson, J.N. orcid.org/0000-0002-6576-3995 et al. (4 more authors) (2020) Equivalent circuit parameter extraction of low-capacitance high-damping PTs. *Electronics Letters*, 56 (7). pp. 347-350. ISSN 0013-5194

<https://doi.org/10.1049/el.2019.3887>

This paper is a postprint of a paper submitted to and accepted for publication in *Electronics Letters* and is subject to Institution of Engineering and Technology Copyright. The copy of record is available at the IET Digital Library: <https://digital-library.theiet.org/content/journals/10.1049/el.2019.3887>

Reuse

Items deposited in White Rose Research Online are protected by copyright, with all rights reserved unless indicated otherwise. They may be downloaded and/or printed for private study, or other acts as permitted by national copyright laws. The publisher or other rights holders may allow further reproduction and re-use of the full text version. This is indicated by the licence information on the White Rose Research Online record for the item.

Takedown

If you consider content in White Rose Research Online to be in breach of UK law, please notify us by emailing eprints@whiterose.ac.uk including the URL of the record and the reason for the withdrawal request.



eprints@whiterose.ac.uk
<https://eprints.whiterose.ac.uk/>

Equivalent circuit parameter extraction of low-capacitance high-damping piezoelectric transformers

J. Forrester, L. Li, J. N. Davidson, M. P. Foster, D. A. Stone, D. C. Sinclair, I. M. Reaney

Abstract: Existing equivalent circuit extraction techniques are inaccurate for piezoelectric transformers with low input capacitance or high damping. A new method is presented, offering improved accuracy in both damping resistance and resonant frequency extraction compared to state-of-the-art methods. Effectiveness is evaluated on two sample PTs, with the proposed method achieving up to 84% decrease in error compared to previous methods.

Introduction: Piezoelectric transformers (PTs), which can replace multiple passive components in low-power resonant converters, offer high power density and efficiency due to their inherent, high-quality mechanical resonance. While presently unable to compete on cost with traditional designs, PTs are non-magnetic and can be designed to operate at high temperature, leading to use in several important applications [1-2].

Most applications of these devices have demanded low damping (hence low loss) and low capacitance (hence easier switching). However, where efficiency is not the primary objective, such as at high temperature or when evaluating multi-modal designs, the assumptions used in existing analysis techniques reduce the accuracy of results. This letter thus proposes an improved technique.



Fig. 1 - BSPT ring-dot PT used in experimental measurements

Piezoelectric transformers use both the direct and inverse piezoelectric effect to transfer energy between the input and output sections of a device. The PT input section is driven by an alternating voltage, resulting in mechanical vibration at its resonant frequency as a result of the inverse piezoelectric effect. This vibration is mechanically coupled with the output section of the device, producing an alternating voltage on the output electrode(s) by the direct piezoelectric effect. Fig. 1 shows a ring-dot PT, where the inner dot acts as the input and the outer ring as the output with a common electrode covering the whole of the base.

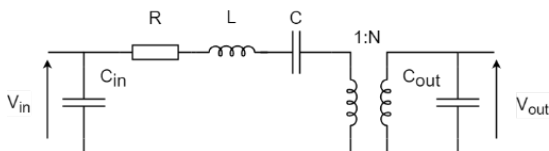


Fig. 2 - Mason equivalent circuit

The Mason equivalent circuit, shown in Fig.2, is used to model the electrical behaviour of the PT when it is operated near the resonant frequency. Whereas the input and output capacitances exist electrically—between the electrodes on the input and output sections—the RLC and ideal transformer collectively model the mechanical behaviour of the PT. An equivalent circuit model is highly beneficial as it allows the simulation of PTs using traditional circuit analysis techniques. The equivalent circuit also provides insight into the expected performance of the PT, with the damping resistance, R , describing the expected losses. However, unlike traditional discrete components, their values cannot be directly measured and, therefore, their values must be estimated.

Several authors have presented techniques for extracting the equivalent circuit parameter values. Ivensky, *et al*, published a technique which uses separate input and output capacitance measurements, along with measurements of the Q-factor, conductance, anti-resonant and resonant

frequencies [3]. Horsely, *et al*, used a curve fitting approach with separate measurements of R and the input and output capacitances, to fit the theoretical gain-frequency curve to the measured curve [4]. Forrester, *et al*, then presented three techniques for parameter extraction [5]. Two of these were improvements over both the approaches by Ivensky, *et al* [3], and Horsley, *et al* [4]. The third was an original method. The three methods were compared, and each proved to be beneficial when applied to a range of PTs for common applications. However, each of the approaches previously published has made the key assumption that $1/(\omega_0 C_{in}) \gg R$ when estimating the value of R itself. In cases where this assumption is invalid, such as in the case of PTs with elevated damping or when analysing modes other than the primary resonance (e.g. spurious modes, which typically have higher damping), none of the methods presented previously are accurate. This situation also arises in the study of dual frequency PTs [6], unoptimised prototype PTs, high temperature PTs and in multi-modal studies which parameterise the Mason equivalent circuit for each mode.

This letter therefore presents an improved method for parameter extraction, suitable for situations where $1/(\omega_0 C_{in}) \gg R$ is invalid.

Limitations of previous approaches: When the output terminals of the PT are short-circuited and the PT is driven at the resonant frequency, the input impedance of the PT is equal to the input capacitance and the damping resistance in parallel:-

$$Z_0 = \frac{RZ_{C_{in}}}{R + Z_{C_{in}}}\bigg|_{\omega=\omega_0} \quad (1)$$

Z_0 is the input impedance of the PT at resonance and $Z_{C_{in}}$, a function of ω , is the impedance of the input capacitor:-

$$Z_{C_{in}} = \frac{-j}{\omega C_{in}} \quad (2)$$

If $1/(\omega_0 C_{in}) \gg R$ is a valid assumption, Z_0 is dominated by the damping resistance and R can be taken as equal to the input impedance. The resonant frequency can also be taken as the frequency at which the input impedance is minimal. However, when $1/(\omega_0 C_{in}) \gg R$ is invalid, R does not dominate the input impedance and, as a result, estimation of R using existing approaches is prone to error. Additionally, and as a consequence, the minimum impedance frequency is no longer the resonant frequency.

This limitation can be illustrated by simulating the input impedance of a PT model with the output shorted. The model's damping resistance is varied through a range of values, and the apparent resonant frequency and damping resistance are extracted using the method employed in [5]. The results of the analysis are shown in Table 1.

Table 1: Error in extracted damping resistance and resonant frequency with changes in true damping resistance relative to input capacitance ($L=10\text{mH}$, $C=50\text{pF}$, $C_{in}=5\text{nF}$, V_{out} short circuited)

$R/ Z_{C_{in}} $		0.1	0.2	1	2	10
Error in R	%	0.99	3.7	38	61	90
	Ω	0.14	1.05	54	172	1275
Error in ω_0	%	<0.01	0.019	0.31	0.75	2.3
	Hz	11	43	687	1681	5099

The results in Table 1 confirm that when $1/(\omega_0 C_{in}) \gg R$ the error is negligible. However, for high R , the extracted values show significant error.

Proposed method: The proposed extraction method uses, as its foundation, method 3 presented by Forrester, *et al* [5]. This method has two elements—component value extraction and ω_0 estimation—both of which are executed simultaneously. In our proposal, we initially assume

ω_0 is known before optimising the extracted component values to find ω_0 .

Component extraction: The input impedance (output shorted) of the PT is measured at two frequencies in the vicinity of the resonant frequency. An expression for the impedance at the two chosen frequencies can be derived by noting that the input impedance, with the output terminals shorted, Z_{OS} , is made up of the input capacitance in parallel with the resonant circuit.

$$Z_{OS} = \frac{Z_{C_{in}} Z_{RLC}}{Z_{C_{in}} + Z_{RLC}} \quad (3)$$

$$Z_{RLC} = R + j\beta \left(\frac{\omega}{\omega_0} - \frac{\omega_0}{\omega} \right) \quad (4)$$

Where β is the reactance of both L and C at the resonant frequency, ω_0 :

$$\beta = \omega_0 L = \frac{1}{\omega_0 C} \quad (5)$$

Substituting (2) and (4) into (3) allows a closed-form expression for the input impedance (output shorted) of a PT (Z_{OS}) to be derived:

$$Z_{OS}(\omega) = \frac{\left(\omega - \frac{\omega_0^2}{\omega} \right) \beta - jR\omega_0}{RC_{in}\omega\omega_0 + j((\omega^2 - \omega_0^2)\beta C_{in} - \omega_0)} \quad (6)$$

The impedance is found for two arbitrarily chosen frequencies, ω_1 and ω_2 . We can write the impedance at these frequencies as Z_1 and Z_2 , respectively.

$$Z_1 = Z_{OS}(\omega_1) = \frac{\left(\omega_1 - \frac{\omega_0^2}{\omega_1} \right) \beta - jR\omega_0}{RC_{in}\omega_1\omega_0 + j((\omega_1^2 - \omega_0^2)\beta C_{in} - \omega_0)} \quad (7)$$

$$Z_2 = Z_{OS}(\omega_2) = \frac{\left(\omega_2 - \frac{\omega_0^2}{\omega_2} \right) \beta - jR\omega_0}{RC_{in}\omega_2\omega_0 + j((\omega_2^2 - \omega_0^2)\beta C_{in} - \omega_0)} \quad (8)$$

It is difficult to measure R accurately independent of our approach, therefore it is beneficial to initially remove it from (7) and (8). At resonance (ω_0), the RLC reduces to just R and the input impedance (output shorted) is equal to the input capacitance and damping resistance in parallel (see (1)). Substituting (2) into (1) and rearranging for R yields:-

$$R = \frac{Z_0}{1 - jC_{in}Z_0\omega_0} \quad (9)$$

Equation (9) is then substituted into (7) and (8).

$$Z_1 = \frac{\left(\omega_1 - \frac{\omega_0^2}{\omega_1} \right) \beta - j \frac{Z_0}{1 - jC_{in}Z_0\omega_0} \omega_0}{\frac{Z_0 C_{in} \omega_1 \omega_0}{1 - jC_{in}Z_0\omega_0} + j((\omega_1^2 - \omega_0^2)\beta C_{in} - \omega_0)} \quad (10)$$

$$Z_2 = \frac{\left(\omega_2 - \frac{\omega_0^2}{\omega_2} \right) \beta - j \frac{Z_0}{1 - jC_{in}Z_0\omega_0} \omega_0}{\frac{Z_0 C_{in} \omega_2 \omega_0}{1 - jC_{in}Z_0\omega_0} + j((\omega_2^2 - \omega_0^2)\beta C_{in} - \omega_0)} \quad (11)$$

Equations (10) and (11) are no longer a function of R but, rather, are a function of Z_0 , which is directly measurable. Equations (10) and (11) can be rearranged for β .

$$\beta = \frac{(C_{in}(\omega_1 - \omega_0)Z_1 Z_0 + j(Z_0 - Z_1))\omega_0 \omega_1}{(1 - C_{in}^2 Z_0 Z_1 \omega_0 \omega_1 + jC_{in}(Z_0 \omega_0 - Z_1 \omega_2))(\omega_1^2 - \omega_0^2)} \quad (12)$$

$$\beta = \frac{(C_{in}(\omega_2 - \omega_0)Z_2 Z_0 + j(Z_0 - Z_2))\omega_0 \omega_2}{(1 - C_{in}^2 Z_0 Z_2 \omega_0 \omega_2 + jC_{in}(Z_0 \omega_0 - Z_2 \omega_2))(\omega_2^2 - \omega_0^2)} \quad (13)$$

Equating (12) and (13) then rearranging yields a polynomial containing C_{in} . After excluding trivial solutions, a quadratic equation remains and is in the form, $aC_{in}^2 + bC_{in} + c = 0$. When solved, there are two solutions for C_{in} in the form $d \pm \sqrt{e}$, only one of which is valid. These solutions have been omitted due to length. Because both d and e are complex, which solution is valid is affected by the location of the complex number branch points and changes dynamically with ω_0 .

Therefore, we will consider C_{in} to have two potentially valid solutions, $\hat{C}_{in} \in \{C_{in<1>}, C_{in<2>}\}$, and determine the correct solution using the method described in the next section.

Given experimental input impedance measurements at the resonant frequency and two neighbouring frequencies (Z_0 , Z_1 and Z_2 respectively), using \hat{C}_{in} leads to two solutions for R from (9), thus $\hat{R} \in \{R_{<1>}, R_{<2>}\}$. Using (12) now provides $\hat{\beta} \in \{\beta_{<1>}, \beta_{<2>}\}$. Where, due to measurement error in Z_0 , Z_1 and Z_2 , any of C_{in} , β or R has an imaginary part, only the real part should be used for solutions.

To determine the correct solution set, the two possibilities are evaluated using an integral sum of squares cost function, $J(\omega_0)$, which has dependency on the unknown resonant frequency ω_0 .

$$\min_{\omega_0, x} J = \int_{\omega_0 - \Delta\omega}^{\omega_0 + \Delta\omega} \left(\frac{|Z_{measured}(\omega)| - |Z_{OS}(\omega, \omega_0, x)|}{|Z_{measured}(\omega)|} \right)^2 d\omega \quad (14)$$

Where $x \in \{\hat{C}_{in}, \hat{R}, \hat{\beta}\}$ and $Z_{measured}$ is the measured input impedance of the PT, with the output shorted, at a range of frequencies in the vicinity of the expected resonance ($\Delta\omega$ is typically around 15% of ω_0). Using (14) and (6) with both possible solution sets for β , C_{in} and R , and experimental measurements of the input impedance over the range of frequencies, yields J . The set of parameters with the lowest cost, yields the best model parameters for a particular value of ω_0 .

Determination of ω_0 : In the methods presented by Ivensky, *et al* [3], Horsley, *et al* [4], and Forrester, *et al* [5], the resonant frequency (ω_0) is taken as the frequency at which input impedance is minimised. This is inaccurate if R is large. However, without prior knowledge of L and C , it is not possible to precisely calculate the resonant frequency and therefore its value has to be estimated.

In our proposal, the minimum impedance frequency is a first approximation for ω_0 . The value of ω_0 is then optimised using (14). The ω_0 value with the overall minimum cost will be the best approximation to β , C_{in} , R and ω_0 . The values of L and C are then calculated using (5).

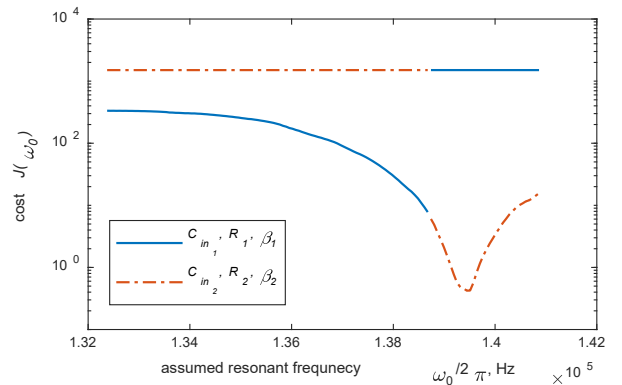


Fig. 3 – Typical output of the cost function J for both solution sets (x) across the range of ω_0 tested. This is the output from the parameter extraction of the BSPT PT discussed in the experimental results and shown in Fig. 4. The discontinuity in the solution is due to the branch point selection in the principal solution for complex square roots.

The range of possible values for ω_0 is constrained since ω_0 must lie between the local minimum and maximum impedances for the mode of interest. Many methods may be used to minimise J ; in our implementation, an exhaustive search was used. An example of the typical output of J , for both sets of x , across the range of ω_0 values examined, is shown in Fig. 3. The overall minimum point on Fig. 3 corresponds to the best model parameters.

Determination of C_{out} and N : The remaining equivalent circuit parameters, C_{out} and N can be found by repeating the same extraction process but with experimental measurements from the output terminals (input shorted) and with C_{out} replacing C_{in} in all relevant equations.

Finally, N can be determined by recognising that:-

$$N = \sqrt{\frac{\beta_{in}}{\beta_{out}}} \quad (15)$$

β_{in} and β_{out} are the β values found from parameter extraction using input and output impedance measurements respectively.

Experimental Results: The equivalent circuit parameters of two sample PTs are extracted to verify the accuracy of the proposed method. Method 3 presented in [5] is also compared. The accuracy of each method is quantified by calculating the root-mean-square error (RMSE) between the theoretical impedance spectra of the parameterised model and the experimentally measured spectra. We calculate error using both linear frequency and impedance.

The first PT under test is a ring-dot PT made from BiScO₃-PbTiO₃ (BSPT), shown in Fig. 1. The PT has a dot radius of 3mm, an inner ring radius of 5mm, an outer radius of 8mm and a thickness of 1mm. The measured and theoretical output impedance spectra (input shorted) produced from both extraction methods are shown in Fig. 4.

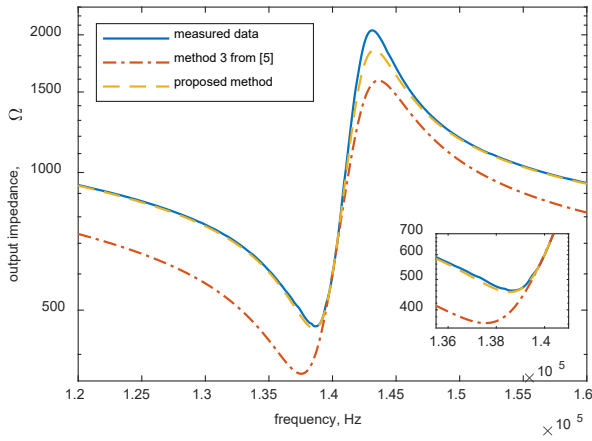


Fig. 4 - Measured and simulated output impedance spectra from the BSPT PT

From the results in Fig. 4, it is clear the proposed method produces a theoretical impedance which is a closer match to the measured response than the state of the art. Whilst the previous method exhibits 180.7 Ω RMSE, the proposed method only exhibits 29.3 Ω RMSE between simulated and measured impedance spectra.

A second PT is also tested. This time, extraction is performed on a spurious resonant mode. The PT under test (TI-PP0361) is a radial mode Transoner PT made from APC841, with dimensions as shown in Fig. 7b of [7]. Extraction is performed on the lowest frequency resonance exhibited by the PT (36 kHz). The resulting measured and simulated input impedance spectra are shown in Fig. 5.

Again, the proposed method produces a more accurate extraction, with the theoretical impedance spectra produced by previous and proposed methods having 114.6 Ω and 22.2 Ω RMSE compared to the measured spectra, respectively.

Discussion: The proposed method produces a more accurate parameter extraction than previous methods. This is particularly clear in the first test, as R is similar in magnitude to $1/(\omega_0 C_{out})$. In the second test, the proposed method again showed improvement over the state of the art, albeit less significant. However, in both cases the simulated impedance from the proposed method still showed some error. This error is inevitable due to model and measurement shortcomings, including non-linearity in the PT and instrumentation noise. However, in the cases we have presented, the effect was small.

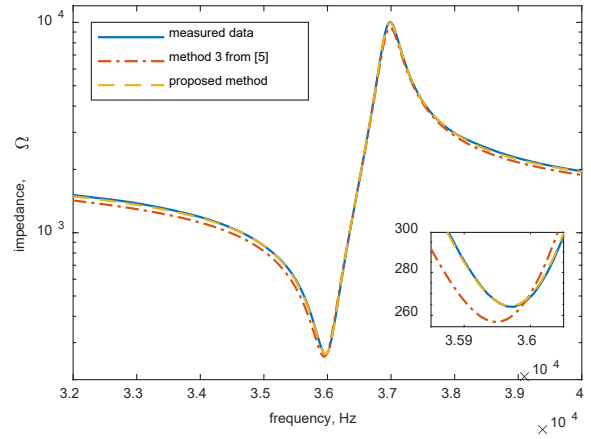


Fig. 5 - Measured and simulated input impedance spectra from the TI-PP0361 PT

Conclusion: An improved method for equivalent circuit parameter extraction from high damping/low capacitance PTs was presented. The proposed method removes a key assumption that is widely used in the literature. The method is experimentally verified against the state of the art and shows increased accuracy of parameter extractions, particularly for PTs with high damping.

J. Forrester, L. Li, J. N. Davidson, M. P. Foster, D. A. Stone, D. C. Sinclair, I. M. Reaney (University of Sheffield, Sheffield, United Kingdom)

Acknowledgement: Supported by the Engineering and Physical Sciences Research Council (EP/P015859/1)

Email: jforrester1@sheffield.ac.uk

References

- [1] M. Ekhtiari, T. G. Zsurzsan, M. A. E. Andersen, and Z. Zhang, "Optimum Phase Shift in the Self-Oscillating Loop for Piezoelectric-Transformer-Based Power Converters," *IEEE Trans. Power Electron.*, vol. 33, no. 9, pp. 8101–8109, Sep. 2018.
- [2] T. Martinez, G. Pillonnet, and F. Costa, "A 15 mV Inductorless Start-up Converter Using a Piezoelectric Transformer for Energy Harvesting Applications," *IEEE Trans. Power Electron.*, vol. 33, no. 3, pp. 2241–2253, 2017.
- [3] G. Ivensky, I. Zafrany, and S. Ben-Yaakov, "Generic operational characteristics of piezoelectric transformers," *IEEE Trans. Power Electron.*, 2002, vol. 17, no. 6, pp. 1049–1057, doi: 10.1109/TPEL.2002.805602
- [4] E. L. Horsley, M. P. Foster, and D. A. Stone, "A frequency-response-based characterisation methodology for piezoelectric transformers," in *2008 2nd Electronics System-Integration Technology Conference*, London, United Kingdom, September 2008, pp. 959–962, doi:10.1109/ESTC.2008.4684481
- [5] J. Forrester, J. Davidson, M. Foster, and D. Stone, "Equivalent Circuit Parameter Extraction Methods for Piezoelectric Transformers", presented at the EPE'19 ECCE Europe, Genoa, Italy, September 2019, pp. 1–10.
- [6] P. Valenta, V. Koucký, and J. Hammerbauer, "Simultaneous power transfer and information transfer via piezoelectric transformer," in *2017 25th Telecommunication Forum (TELFOR)*, Belgrade, Serbia, November 2017, pp. 1–4, doi:10.1109/TELFOR.2017.8249412
- [7] M. P. Foster, J. N. Davidson, E. L. Horsley, and D. A. Stone, "Critical Design Criterion for Achieving Zero Voltage Switching in Inductorless Half-Bridge-Driven Piezoelectric-Transformer-Based Power Supplies," *IEEE Trans. Power Electron.*, vol. 31, no. 7, pp. 5057–5066, Jul. 2016.